

Pharmacophore Modeling of Substituted 1,2,4-Trioxanes for Quantitative Prediction of their Antimalarial Activity[†]

Amit K. Gupta,[‡] S. Chakroborty,[‡] Kumkum Srivastava,[§] Sunil K. Puri,[§] and Anil K. Saxena^{*,‡}

Medicinal and Process Chemistry Division and Parasitology Division, Central Drug Research Institute, CSIR, Lucknow, 226001, India

Received May 8, 2010

A pharmacophore model has been developed for determining the essential structural requirements for antimalarial activity from the eight series of substituted 1,2,4-trioxanes. The best pharmacophore model possessing two aliphatic hydrophobic, one aromatic hydrophobic, one hydrogen-bond (H-bond) acceptor, and one H-bond acceptor (lipid) feature for antimalarial activity showed an excellent correlation coefficient for the training ($r^2_{\text{training}} = 0.85$) and a fair correlation coefficient for the test set ($r^2_{\text{test}} = 0.51$) molecules. The model predicts well to other known substituted 1,2,4-trioxanes including those which either are drugs or are undergoing clinical trials. In order to further validate this model, five substituted 1,2,4-trioxanes were synthesized from the generated focused library and screened for antimalarial activity. The observed activity of these molecules was consistent with the pharmacophore model, suggesting that the model may be useful in the design of potent antimalarial agents.

1. INTRODUCTION

In spite of worldwide efforts to combat malaria, approximately 247 million malaria cases were reported in 2006, causing nearly a million deaths, with the majority in children under five years.¹ According published reports, 109 countries were found endemic for malaria in 2008,¹ and even in 2009, the disease was responsible for a child's death every 30 s.^{2,3} The major problem in the chemotherapy of malaria is the development of resistance of the *Plasmodium falciparum* malaria parasites to many of the standard quinoline antimalarial drugs, like chloroquine.⁴

The discovery of artemisinin, an active principle of the Chinese traditional drug Qinghaosu extracted from the plant *Artemisia annua*, has opened a new era in the malarial chemotherapy. Artemisinin and its more potent analogues viz. artemether, arteether (Figure 1), and artesunic acid represent the endoperoxide class of compounds which are highly active against both chloroquine-sensitive and -resistant strains of *P. falciparum*.⁵ These fast-acting drugs are suitable for the treatment of cerebral malaria caused by multidrug-resistant *P. falciparum*.^{6–8}

Although the first incidence of stable artemisinin resistance was reported in 2006 by Cravo et al.⁹ and thereafter in December 2008, both were in the western part of Cambodia,¹⁰ and there is no evidence of artemisinin resistance occurring anywhere else in the world. The World Health Organization (WHO)-recommended artemisinin combination therapy (ACT) is the best option available to date for the chemotherapy of malaria, and according to a study carried out by Maude et al., immediate implementation of ACT may

eliminate artemisinin-resistant malaria in less than five years in Cambodia.¹¹

The exact mode of action of artemisinin and its analogues is still unknown. However, one of the widely known mechanisms is that, during the erythrocytic stage of the parasite life cycle, iron(II) liberated during hemoglobin degradation¹² reduces the peroxide bond in the 1,2,4-trioxane to form a sequentially highly unstable oxygen (O)-centered radical, which then rearranges to a more stable carbon (C)-centered free radical, high-valent iron oxo species, and reactive epoxides. These reactive intermediates alone, or in combination, kill the parasite, possibly by disrupting the vital biochemical processes or by alkylating or oxidizing the critical biomolecules.¹³ Others have argued that endoperoxide cleavage is catalyzed by a cytoplasmic iron(II) source. The resulting reactive species then specifically inhibits an adenosine 5'-triphosphate-dependent (ATP-dependent) Ca^{2+} pump called PfATP6 located on the endoplasmic reticulum and results in killing the parasite.¹⁴

The major drawback of all semisynthetic trioxanes is that their synthesis needs artemisinin as a starting material, and currently the production of artemisinin from natural source remains relatively low. To address the supply issue, a number of groups have attempted to produce totally synthetic 1,2,4-trioxane analogues, some of which have demonstrated remarkable antimalarial activity,^{15–19} while Vennerstrom and co-workers have reported the first 1,2,4-trioxolane endop-

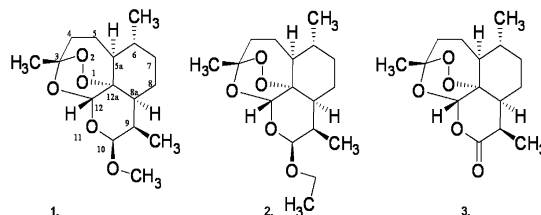


Figure 1. (1) Artemether, (2) arteether, and (3) artemisinin.

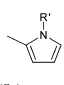
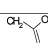
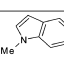
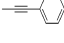
* Corresponding author. E-mail: anilsak@gmail.com. Telephone: +9152226124112/ex 4386. Fax: +9152226123405.

[†] CDRI communication no. 7888.

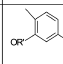
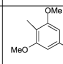
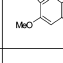
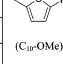
[‡] Medicinal and Process Chemistry Division.

[§] Parasitology Division.

Table 1. Structures of the Molecules Used in Training and Test Sets^a

| C.N. | X | R | C.N. | X | R |
|------|---|--|------|---|--|
| 1* | - | Ph (C ₁₂ -OMe) α | 45* | - |  R' = Me R' = PhCH ₂ R' =  R' = EtOOCH ₂ |
| 2* | - | p-PhPh (C ₁₂ -OMe) α | 46 | - | |
| 3* | - | p-PhPh (C ₁₂ -OMe) β | 47 | - | |
| 4 | - | 1-naphthyl (C ₁₂ -OMe) α | 48* | - | |
| 5* | - | 1-naphthyl (C ₁₂ -OMe) β | 49 | - |  (C ₁₀) α |
| 6 | - | p-ClPh (C ₁₂ -OMe) α | 50 | - |  R' = Cl R' = F R' = SMe |
| 7 | - | p-ClPh (C ₁₂ -OMe) β | 51 | - | |
| 8* | - | 2-furyl (C ₁₂ -OMe) α | 52* | - | |
| 9* | - | p-HOCH ₂ Ph (C ₁₂ -OMe) α | 53 | - | 2'-thiazolyl |
| 10 | - | p-HOCH ₂ Ph (C ₁₂ -OMe) β | 54* | - | 2'-benzothiazolyl |
| 11 | - | p-MeOCH ₂ Ph (C ₁₂ -OMe) α | 55 | - | -CHO |
| 12* | - | p-MeOCH ₂ Ph (C ₁₂ -OMe) β | 56 | - | -C(O)Me-Bu |
| 13* | - | p-MeO(O)OCH ₂ Ph (C ₁₂ -OMe) α | 57* | - | -C(O)Ph |
| 14* | - | p-MeC(O)OCH ₂ Ph (C ₁₂ -OMe) α | 58* | - | -C(OH)Ph ₂ |
| 15 | - | p-MeC(O)OCH ₂ Ph (C ₁₂ -OMe) β | 59 | - | -CH=CH ₂ |
| 16 | - | p-(p'-FPhCH ₂ OCH ₂)Ph (C ₁₂ -OMe) α | 60* | - | E-CH=CHPh |
| 17* | - | p-(p'-FPhCH ₂ OCH ₂)Ph (C ₁₂ -OMe) β | 61* | - | Z-CH=CHPh |
| 18* | - | p-FPh (C ₁₂ -OMe) α | 62 | - | E-CH=CHPhNO ₂ -p |
| 19* | - | p-FPh (C ₁₂ -OMe) β | 63 | - | Z-CH=CHPhNO ₂ -p |
| 20 | - | p-F-o-MePh (C ₁₂ -OMe) α | 64* | - | -SPh (C ₁₂ -R)β |
| 21 | - | p-F-o-MePh (C ₁₂ -OMe) β | 65* | - | -SO ₂ Ph (C ₁₂ -R)β |
| 22 | - | p-CF ₃ Ph (C ₁₂ -OMe) α | 66 | - | -SO ₂ Ph (C ₁₂ -R)α |
| 23 | - | p-CF ₃ Ph (C ₁₂ -OMe) β | 67* | - | -SPh-OMe-p (C ₁₂ -R)β |

^a C. N. = compound name, and compounds marked with asterisk (*) are training set molecules, while the remaining are test set molecules.

| C.N. | X | R | C.N. | X | R |
|------|--------------------|--|------|--|---|
| 24* | - | CF ₃ CH ₂ CH ₂ - (C ₁₂ -OMe) β | 68 | - | -SO ₂ Ph-OMe-p (C ₁₂ -R) β |
| 25* | - | FCH ₂ - (C ₁₂ -OMe) α | 69* | - | -SO ₂ Ph-OMe-p (C ₁₂ -R)α |
| 26* | - | FCH ₂ - (C ₁₂ -OMe) β | 70* | - | -SPh-Cl-p (C ₁₂ -R) β |
| 27 | Ph | -CH ₂ CH ₂ OH | 71* | - | -SO ₂ Ph-Cl-p (C ₁₂ -R) β |
| 28 | Me ₂ Si | -CH ₂ CH ₂ OH | 72 | - | -SO ₂ Ph-Cl-p (C ₁₂ -R) α |
| 29 | Ph | H | 73* | - | OHCH ₂ CH ₂ - Me (C ₄ -R) β |
| 30* | - | Me | 74* | - | OHCH ₂ CH ₂ - Me (C ₄ -R) α |
| 31 | - | Et | 75 | - | OHCH ₂ CH ₂ - PhCH ₂ - (C ₄ -R) β |
| 32 | - | (CH ₃) ₂ CHCH ₂ CH ₂ | 76* | - | OHCH ₂ CH ₂ - H |
| 33 | - | PhCH ₂ CH ₂ CH ₂ | 77 | - | OHCH ₂ CH ₂ - PhCH ₂ - (C ₄ -R) β |
| 34 | - | CH ₂ =CH- | 78* | H | Ph (C ₄ -R) β |
| 35 | - | Ph | 79* | H | OHCH ₂ - (C ₄ -R) β |
| 36* | - |  (C ₁₀ -OMe) α | 80* | H | p-(HOCH ₂)PhCH ₂ - |
| 37* | - | Allyl | 81 | H | (PhO) ₂ P(O)OCH ₂ CH ₂ - |
| 38* | - |  (C ₁₀ , OMe) α | 82* | H | PhCH ₂ OCH ₂ CH ₂ - |
| 39 | - |  (C ₁₀ -OMe) α | 83* | H | p-FPhCH ₂ OCH ₂ CH ₂ - |
| 40* | - | H | 84 | -CH ₃ | (PhO) ₂ P(O)OCH ₂ CH ₂ - |
| 41 | - | Me | 85* | -CH ₃ | PhCH ₂ OCH ₂ CH ₂ - |
| 42 | - | Et | 86* | -CH ₃ | p-FPhCH ₂ OCH ₂ CH ₂ - |
| 43 | - | t-butyl | 87 | -CH ₂ O p-(FPhCH ₂) | H |
| 44* | - |  (C ₁₀ -OMe) α | 88 | -CH ₂ Ph p-[CH ₂ O- p-(FPhCH ₂)] | H |

eroxide, OZ-277, which has recently entered into clinical trials.²⁰ However, according to Uhlemann and co-worker, although the mode of action of both types of antimalarials (artemisinins and OZ-277) are similar in many aspects, as both concentrate in intraerythrocytic parasites 200-300 fold compared with extracellular concentrations, there are also remarkable differences in their behavior particularly in the potency to inhibit PfATP6 and the variability of OZ-277 in the subcellular localization pattern.²¹

Few comparative molecular field analysis (CoMFA) studies on the artemisinin derivatives have been reported,^{22,23} and a pharmacophore model was developed by Grigorov et al. using bi- and tricyclic 1,2,4-trioxanes as antimalarial agents.²⁴ But to date, no pharmacophore modeling study has been reported on the artemisinin family of substituted 1,2,4-trioxanes.

Considering the importance of artemisinin and its analogues as a potent class of antimalarial drugs effective against the multidrug-resistant *P. falciparum* strains and unavailability of the exact target for this class of molecule,²⁵ it appeared of interest to develop a pharmacophore model for determining the essential structural requirements for this class of molecules for their antimalarial activity. Such a model may be useful in designing of this class of molecules for antimalarial activity. The development and validation of such a model is presented in this paper.

2. RESULTS AND DISCUSSION

2.1. Pharmacophore Description. The QSAR studies were performed using eight series of substituted 1,2,4-trioxanes comprising 88 artemisinin analogues (activity ranges from 1.4 to 2000 nM) reported in literature²⁶⁻³¹ by adopting the HypoGen algorithm³² of CATALYST. The

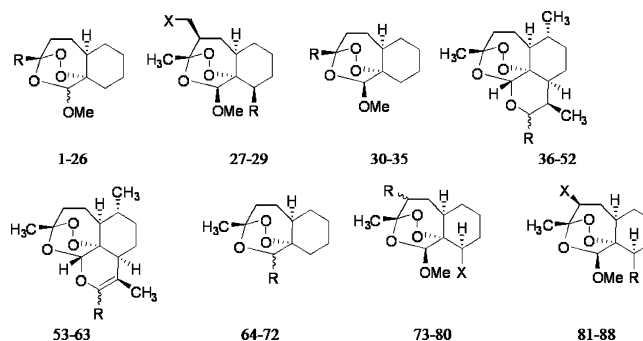


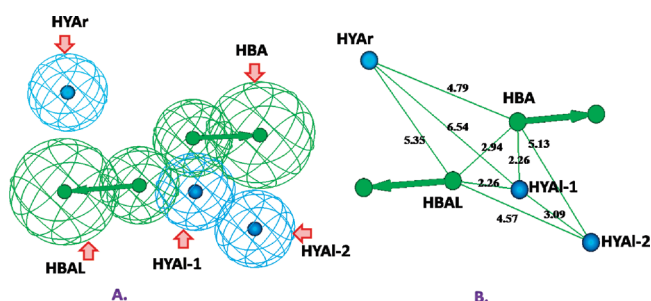
Figure 2. Common structures of molecules used in pharmacophore study.

homogeneity of the biological assays is one of the important aspects in quantitative structure–activity relationship (QSAR) studies, therefore, the data set was collected from the same research group following the same biological testing protocol and were rationally divided into a training set of 45 compounds (marked with an asterisk in Table 1) and a complementary test set of 43 compounds according to published guidelines.³³ The structures of test and training set molecules have been given in Figure 2 and Table 1.

The HypoGen algorithm of CATALYST resulted in the generation of 10 alternative pharmacophores describing the antimalarial activity of the training set compounds. The details of the pharmacophore generation procedure have been described in the Experimental Section of this manuscript. The quality of the generated pharmacophore hypotheses were evaluated by considering the cost functions calculated by the HypoGen module during hypothesis generation. The composition (in terms of chemical features that are necessary for activity), ranking score, and statistical parameters associated with the hypotheses are reported in Table 2.

Table 2. Composition (Features), Cost (Bits), and Statistical Parameters (Rmsd and Correlation) Associated with the 10 Best Hypotheses (Pharmacophore Models)

| serial no. | hypothesis | features ^a | total cost | Δcost^b | rmsd | correlation (R) |
|------------|------------|------------------------|------------|-----------------------|------|-----------------|
| 1 | Hypo 1 | HBA, HBAL, 2HYAl, HYAr | 174.7 | 28.81 | 0.60 | 0.92 |
| 2 | Hypo 2 | HBA, HBAL, HYAl, HYAr | 181.8 | 21.7 | 0.80 | 0.86 |
| 3 | Hypo 3 | HBA, HBAL, 2HYAl, HYAr | 183.1 | 20.4 | 0.85 | 0.83 |
| 4 | Hypo 4 | HBA, HBAL, HYAl, HYAr | 184.6 | 18.9 | 0.88 | 0.82 |
| 5 | Hypo 5 | HBA, HBAL, 2HYAl, HYAr | 185.2 | 18.3 | 0.86 | 0.82 |
| 6 | Hypo 6 | HBA, HBAL, 2HYAl, HYAr | 185.3 | 18.2 | 0.83 | 0.84 |
| 7 | Hypo 7 | HBA, HBAL, 2HYAl, HYAr | 185.5 | 18 | 0.84 | 0.84 |
| 8 | Hypo 8 | HBA, HBAL, HYAl, HYAr | 185.6 | 17.9 | 0.86 | 0.82 |
| 9 | Hypo 9 | HBA, HBAL, HYAl, HYAr | 186.0 | 17.5 | 0.89 | 0.81 |
| 10 | Hypo 10 | HBA, HBAL, 2HYAl, HYAr | 186.1 | 17.4 | 0.93 | 0.80 |

^a HBA: hydrogen-bond acceptor, HBAL: hydrogen-bond acceptor lipid, HYAl: hydrophobic aliphatic, and HYAr: hydrophobic aromatic.^b $\Delta\text{cost} = (\text{null cost} - \text{total cost})$.**Figure 3.** (A) Three dimensional arrangement of pharmacophoric features generated from the training set of 45 substituted 1,2,4-trioxanes; HBA and HBAL as green, HYAl-1 and HYAl-2 as dark blue; and HYAr as light blue. (B) Interfeature distance between different features in the pharmacophore model.

The fixed cost of the 10 top-scored hypotheses was 166.6 bits, well separated from the null hypothesis cost of 203.5 bits. The top-ranked pharmacophore model (Hypo-1) had the best predictive power and statistical significance described by the high correlation coefficient ($r^2_{\text{training}} = 0.85$), low root-mean-square deviation (rmsd, 0.60), weight (1.13) and error (159.403) costs and a cost difference of 28.81, satisfying the acceptable range recommended in the cost analysis of the CATALYST procedure.³³ The configuration cost was 14.15, indicating that all generated models have been thoroughly analyzed. The cost difference between total and fixed costs for the best hypothesis was only 8.0 bits, indicating the high probability of the true correlation of the data. It is due to the fact that the lower the cost difference between the total and fixed costs, the higher the probability is for the true correlation of the data. Thus Hypo-1 was retained for further analysis as the best pharmacophore model for antimalarial activity with five features, viz., one H-bond acceptor (HBA), one H-bond acceptor lipid (HBAL), two aliphatic hydrophobic (HYAl), and one aromatic hydrophobic (HYAr) function at specific geometric locations in three-dimensional (3D) space (Figure 3A) and is also statistically the most relevant model. The interfeature distance between all these features has been shown in Figure 3B.

The pharmacophore model mapped very well to the training set molecules. The observed IC_{50} along with predicted IC_{50} values for the antimalarial activity of the training set compounds are given in Table 3.

A plot between the pIC_{50} values of observed versus estimated activity demonstrated a good correlation coefficient ($r^2_{\text{training}} = 0.85$) for training set molecules within the range

of uncertainty 3, indicating the high predictive ability of the pharmacophore (Figure 4).

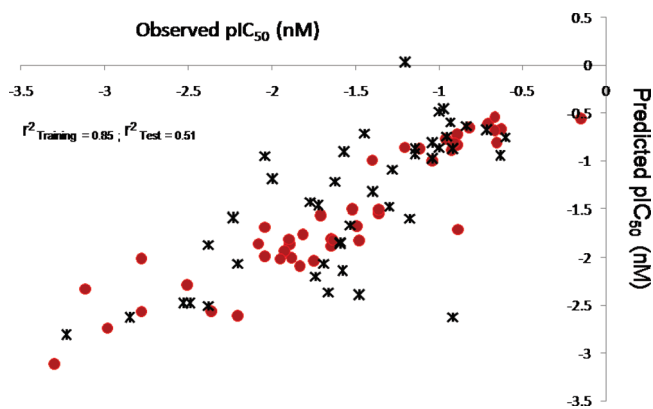
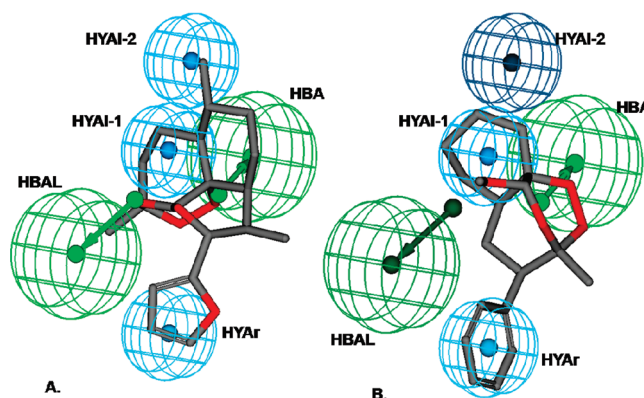
Previously a four feature hypothesis was reported by Grigorov et al. using bi- and tricyclic 1,2,4-trioxanes, viz., one HBD, one HBA, and two HY features for the antimalarial activity.²⁴ Comparison of the above hypothesis with our model depicted well-differentiated hydrophobic features (two HYAl and one HYAr) with an additional HBAL feature. However, the HBD feature was absent in our model, which may be due to the absence of such functional groups in the training set molecules. Although there are two CoMFA and comparative molecular similarity indices analysis (CoMSIA) studies have been reported earlier using semisynthetic derivatives of artemisinin,^{22,23} their findings vary in terms of steric and electrostatic contours distribution around the molecule. These variations may be due to the limitations of CoMFA and CoMSIA studies, as they are highly specific to the molecular alignment. However, our study corroborates with a study carried out by Jung et al. in terms of HYAl feature location in a 3D space, where they described the favorable steric bulk requirement, and corroborates with both studies in terms of HBA feature location, where the favorable partial negative charge requirement near the peroxide group of trioxane moiety has been described for antimalarial activity of artemisinin analogues.

Pharmacophoric representation of the most potent compound 40 of the data set showed the presence of 2-furyl group at C-10 position provided HYAr function to the molecule, whereas the trioxanes ring provided HBA and HBAL function (Figure 5A). The three chain carbon linked with the C-3 and C-12a positions of the trioxane ring and the methyl group at C-6 position of the molecule 40 provided the HYAl-1 and HYAl-2 functions, respectively, to the molecule. The same study carried with the least active compound of the data set 78 ($\text{IC}_{50} = 2000 \text{ nM}$) depicted the absence of HYAl-2 function mapping due to absence of an alkyl group at the C-6 position of the molecule, while at the same time, the molecule failed to access the HBAL feature in order to fit other features of the pharmacophore (Figure 5B).

It has been observed from the mapping of the training set molecules to the pharmacophore that, among all the active trioxanes, the peroxide group of trioxane ring provided a HBA feature, while the oxygen atom at position 4 of 1,2,4-trioxane motif provided a HBAL feature. The importance of peroxide group in trioxane moiety is well-known since it

Table 3. Observed and Predicted Activity Values of the Compounds in the Training Set

| serial no. | comp. name | obs. activity (IC ₅₀) nM | pred. activity (IC ₅₀) nM | obs. activity (pIC ₅₀) nM | pred. activity (pIC ₅₀) nM | error ^a | obs. activity scale ^b | pred. activity scale |
|------------|------------|---|--|--|---|--------------------|-------------------------------------|-------------------------|
| 1 | 1 | 110 | 97.17 | -2.04 | -1.99 | -1.13 | ++ | ++ |
| 2 | 2 | 76 | 101.46 | -1.88 | -2.01 | 1.33 | ++ | ++ |
| 3 | 3 | 68 | 123.26 | -1.83 | -2.09 | 1.81 | ++ | ++ |
| 4 | 5 | 44 | 64.12 | -1.64 | -1.81 | 1.45 | +++ | ++ |
| 5 | 8 | 600 | 102.89 | -2.78 | -2.01 | -5.83 | + | ++ |
| 6 | 9 | 78 | 73.32 | -1.89 | -1.87 | -1.06 | ++ | ++ |
| 7 | 12 | 51 | 36.67 | -1.71 | -1.56 | -1.39 | ++ | +++ |
| 8 | 13 | 79 | 65.19 | -1.9 | -1.81 | -1.21 | ++ | ++ |
| 9 | 14 | 44 | 76.33 | -1.64 | -1.88 | 1.73 | +++ | ++ |
| 10 | 17 | 23 | 35.17 | -1.36 | -1.55 | 1.53 | +++ | +++ |
| 11 | 18 | 65 | 57.99 | -1.81 | -1.76 | -1.12 | ++ | ++ |
| 12 | 19 | 30 | 66.82 | -1.48 | -1.82 | 2.22 | +++ | ++ |
| 13 | 24 | 84 | 85.74 | -1.92 | -1.93 | 1.02 | ++ | ++ |
| 14 | 25 | 320 | 194.77 | -2.51 | -2.29 | -1.64 | + | + |
| 15 | 26 | 160 | 406.55 | -2.2 | -2.61 | 2.54 | + | + |
| 16 | 30 | 960 | 549.03 | -2.98 | -2.74 | -1.74 | + | + |
| 17 | 36 | 4.2 | 4.7 | -0.62 | -0.67 | 1.12 | +++ | +++ |
| 18 | 37 | 6.6 | 4.53 | -0.82 | -0.66 | -1.46 | +++ | +++ |
| 19 | 38 | 7.8 | 5.33 | -0.89 | -0.73 | -1.47 | +++ | +++ |
| 20 | 40 | 1.4 | 3.63 | -0.15 | -0.56 | 2.59 | +++ | +++ |
| 21 | 44 | 5.1 | 4.13 | -0.71 | -0.62 | -1.23 | +++ | +++ |
| 22 | 45 | 4.6 | 3.49 | -0.66 | -0.54 | -1.32 | +++ | +++ |
| 23 | 48 | 9.1 | 5.94 | -0.96 | -0.77 | -1.53 | +++ | +++ |
| 24 | 52 | 8.4 | 7.79 | -0.92 | -0.89 | -1.07 | +++ | +++ |
| 25 | 54 | 7.8 | 6.84 | -0.89 | -0.84 | -1.14 | +++ | +++ |
| 26 | 57 | 4.6 | 4.85 | -0.66 | -0.69 | 1.05 | +++ | +++ |
| 27 | 58 | 4.5 | 6.49 | -0.65 | -0.81 | 1.45 | +++ | +++ |
| 28 | 60 | 16 | 7.27 | -1.2 | -0.86 | -2.19 | +++ | +++ |
| 29 | 61 | 8.1 | 6.55 | -0.91 | -0.82 | -1.23 | +++ | +++ |
| 30 | 64 | 56 | 108.97 | -1.75 | -2.04 | 1.94 | ++ | ++ |
| 31 | 65 | 33 | 31.82 | -1.52 | -1.5 | -1.03 | +++ | +++ |
| 32 | 67 | 89 | 104.13 | -1.95 | -2.02 | 1.17 | ++ | ++ |
| 33 | 69 | 43 | 66.16 | -1.63 | -1.82 | 1.53 | ++ | ++ |
| 34 | 70 | 110 | 48.62 | -2.04 | -1.69 | -2.26 | ++ | +++ |
| 35 | 71 | 23 | 32.14 | -1.36 | -1.51 | 1.39 | +++ | +++ |
| 36 | 73 | 7.7 | 51.47 | -0.89 | -1.71 | 6.68 | +++ | ++ |
| 37 | 74 | 1300 | 214.34 | -3.11 | -2.33 | -6.06 | + | + |
| 38 | 76 | 120 | 72.56 | -2.08 | -1.86 | -1.65 | ++ | ++ |
| 39 | 78 | 2000 | 1299.85 | -3.3 | -3.11 | -1.53 | + | + |
| 40 | 79 | 230 | 364.19 | -2.36 | -2.56 | 1.58 | + | + |
| 41 | 80 | 600 | 368.25 | -2.78 | -2.57 | -1.63 | + | + |
| 42 | 82 | 25 | 9.92 | -1.4 | -1 | -2.52 | +++ | +++ |
| 43 | 83 | 31 | 47.45 | -1.49 | -1.68 | 1.53 | ++ | ++ |
| 44 | 85 | 11 | 10.03 | -1.04 | -1 | -1.1 | +++ | +++ |
| 45 | 86 | 13 | 7.5 | -1.11 | -0.88 | -1.73 | +++ | +++ |

^a Values in the error column represent the ratio of predicted activity to observed activity, or its negative inverse if the ratio is less than 1.^b Activity scale: highly active (<50 nM, +++), moderately active (51–200 nM, ++), and less active (>200 nM, +).**Figure 4.** Correlation displaying the observed versus estimated pIC₅₀ (nM) values in the 0 to -3.5 range for the training set of 45 (shown in red color) and test set of 43 molecules (shown in black color).**Figure 5.** (A) Mapping of the most active compound of the data set 40 onto the pharmacophore. (B) Pharmacophore mapping of the least potent analogue of the data set 78 showing two missed features of the pharmacophore, i.e., HBAL and HYAI-2 (shown as nonhighlighted features).

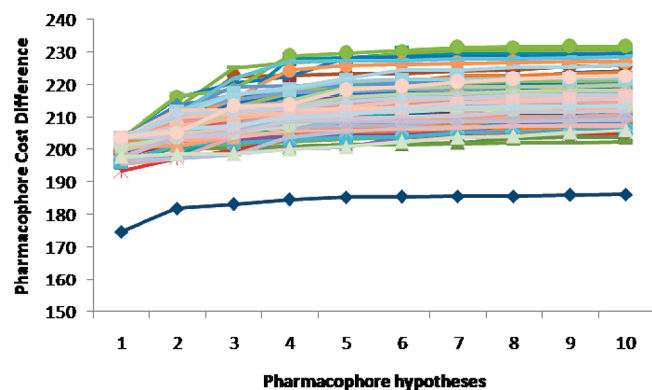


Figure 6. The cost difference of between the Hypo-1 (blue color) and the scrambled runs (other colors).

is responsible for the generation of free radicals. A study led by Wei et al. has shown that artemisinin treatment of membranes (especially in the presence of heme) can cause lipid damage.³⁴ The oxygen atom at position 4 in the 1,2,4-trioxane moiety seemed to be important in this context, as described by the lipid kind of HBAL feature of the pharmacophore as it may cause the phospholipid instability and the membrane damage in the parasite. In view of above, it may be concluded that both of these features are crucial for antimalarial activity of substituted 1,2,4-trioxane molecules. Further, on the basis of the mapping experiment of the training set molecules, it may be concluded that the addition of a bulky aliphatic group at the region joining C-3 to C-12a and C-6 positions, while addition of aromatic groups at C-10 position of the substituted 1,2,4-trioxanes, may lead to a significant increase in antimalarial activity.

2.2. Evaluation of the Hypogen Model. **2.2.1. Score Hypothesis.** The training set was submitted to a score hypothesis process. Within this procedure, the activity of every single training set molecule was estimated by the hypothesis. The actual and estimated antimalarial activity of the 45 training set compounds based on Hypo-1 are listed in Table 3, where 42 molecules out of the 45 in the training set have errors less than 3, and only three molecules (8, 73, and 74) have errors less than 7, confirming that our hypothesis is a reliable model for describing the structure–activity relationship (SAR) in the training set.

2.2.2. Cat Scramble Validation (Fisher Test). To evaluate the statistical relevance of the model, the Fisher's randomization test has been applied. This test involves thorough randomization of the training set to validate and derive the significance of the generated best model. As a consequence, the pharmacophore model corresponding to the Hypo-1 was evaluated for the statistical significance using a randomization trial procedure derived from the Fisher method.³⁵ These randomized spreadsheets should yield hypotheses with lesser statistical significance than the original model to suggest that the original hypothesis represents a true correlation. The number of such random trials depends on what level of statistical significance is to be achieved. For a 95% confidence level, 19 spreadsheets are created, while for 98% and 99% confidence levels, 49 and 99 spreadsheets are created, respectively. Our model was found to be 99% significant in the F-randomization test which substantiates the significance of the model (Figure 6).

2.3. Test Set Validation. The robustness of the generated model was further assessed by its predictability on the test

set containing 43 substituted 1,2,4-trioxanes. The observed IC_{50} along with predicted IC_{50} values of the test set compounds are given in Table 4. The overall correlation coefficient value of ($r^2_{test} = 0.51$) between the observed and estimated activity of the 43 test set molecule was indicative of its good predictive quality (Figure 4). Among the test set molecules, the molecule 27 (obs. act 8.2 and pred. act ~422) has shown maximum deviation in our QSAR analysis. This compound had also shown high activity as compared to its other closely related structural analogues in the reported paper.²⁶ Its removal improved the r^2 value from 0.51 to 0.61. This molecule follows the same pharmacophore mapping trend as others of its series analogues, where it has also missed the HBAL and HYA1-2 feature. The poor prediction (poor mapping) of this molecule seemed to be due to the inability of these molecules to achieve an energetically favorable conformation as well as the interfeature distances (geometrical distance) between the important features found in the best pharmacophore.

In the most potent analogue of the test set 49, the trioxane ring provided HBA and HBAL features, while the three chain carbon linked with the C-3 and C-12a positions and the methyl group at C-6 of the 49 provided the HYA1–1 and HYA1-2 functions, respectively, to the molecule. The missed HYAr feature was compensated by the high-fitted score values of other essential features, viz., one HBAL, one HBA, and two HYA1, for ranking this molecule as active. The least potent member of the test set (75) failed to map the HYAr and HYA1-1 features of the hypothesis completely and hence was ranked as least active.

2.4. External Test Set Validation. **2.4.1. Validation through Known Synthetic Substituted 1,2,4-Trioxanes.** As the main purpose of the quantitative model is to identify the active structures through virtual screening, hence to check the predictive ability of the pharmacophore model, an external data set comprising first-, second-, and third-generation synthetic substituted 1,2,4-trioxanes³⁶ was submitted to pharmacophore mapping. External test set molecules, along with their observed and predicted activity, have been given in Table 5, where the predicted values well described the observed antimalarial activity of these compounds.

2.4.2. Validation of the Generated Hypothesis for Its Predictability against Clinically Active Trioxanes. The validity of this pharmacophore model was further examined on highly active trioxane molecules which either are drugs or are undergoing clinical trials, viz., artemisinin,²⁶ artemether,³⁷ arteether,²⁶ artesunate,²¹ artelinate, and artemisone.³⁸ The observed and predicted activity of these molecules are listed in Table 6. Interestingly these molecules mapped well to the features of the best hypotheses, and the model also ranked them as active. Since the model discriminated well between active and inactive, it may be considered for virtual screening to prioritize the molecules for the synthesis and evaluation as antimalarial agents.

The poor predicted values for two compounds of the external test set and for artemisone of the clinically active compounds may be due to the following reasons. The biological activity of these molecules has come from different research groups/laboratories and has not been determined under similar conditions than those of training set molecules, hence the chances of error are expected in their activity

Table 4. Observed and Predicted Activity Values of the Compounds in the Test Set

| serial no. | comp. name | obs. activity (IC ₅₀) nM | pred. activity (IC ₅₀) nM | obs. activity (pIC ₅₀) nM | pred. activity (pIC ₅₀) nM | error ^a | obs. activity scale ^b | pred. activity scale |
|------------|------------|---|--|--|---|--------------------|-------------------------------------|-------------------------|
| 1 | 4 | 170 | 38.99 | -2.23 | -1.59 | -4.36 | ++ | +++ |
| 2 | 6 | 49 | 116.01 | -1.69 | -2.06 | 2.37 | +++ | ++ |
| 3 | 7 | 55 | 158.42 | -1.74 | -2.2 | 2.88 | ++ | ++ |
| 4 | 10 | 15 | 39.23 | -1.18 | -1.59 | 2.61 | +++ | +++ |
| 5 | 11 | 39 | 68.76 | -1.59 | -1.84 | 1.76 | +++ | ++ |
| 6 | 15 | 20 | 29.87 | -1.30 | -1.48 | 1.49 | +++ | +++ |
| 7 | 16 | 42 | 16.38 | -1.62 | -1.21 | -2.56 | +++ | +++ |
| 8 | 20 | 99 | 15.43 | -2 | -1.19 | -6.42 | ++ | +++ |
| 9 | 21 | 34 | 46.12 | -1.53 | -1.66 | 1.36 | +++ | +++ |
| 10 | 22 | 39 | 71.72 | -1.59 | -1.86 | 1.84 | +++ | ++ |
| 11 | 23 | 53 | 28.97 | -1.72 | -1.46 | -1.83 | ++ | +++ |
| 12 | 27 | 8.3 | 422.73 | -0.92 | -2.63 | 50.93 | +++ | + |
| 13 | 28 | 240 | 319.77 | -2.38 | -2.5 | 1.33 | + | + |
| 14 | 29 | 340 | 301.95 | -2.53 | -2.48 | -1.13 | + | + |
| 15 | 31 | 710 | 425.1 | -2.85 | -2.63 | -1.67 | + | + |
| 16 | 32 | 160 | 115.84 | -2.2 | -2.06 | -1.38 | ++ | ++ |
| 17 | 33 | 110 | 8.87 | -2.04 | -0.95 | -12.41 | ++ | +++ |
| 18 | 34 | 46 | 232.44 | -1.66 | -2.37 | 5.05 | +++ | + |
| 19 | 35 | 38 | 138.55 | -1.58 | -2.14 | 3.64 | +++ | ++ |
| 20 | 39 | 9 | 5.55 | -0.95 | -0.74 | -1.62 | +++ | +++ |
| 21 | 41 | 5.2 | 4.76 | -0.72 | -0.68 | -1.09 | +++ | +++ |
| 22 | 42 | 8.6 | 3.93 | -0.93 | -0.59 | -2.19 | +++ | +++ |
| 23 | 43 | 10 | 3.06 | -1 | -0.49 | -3.27 | +++ | +++ |
| 24 | 46 | 16 | 0.93 | -1.2 | 0.03 | -17.26 | +++ | +++ |
| 25 | 47 | 9.4 | 2.87 | -0.97 | -0.46 | -3.27 | +++ | +++ |
| 26 | 49 | 4 | 5.67 | -0.6 | -0.75 | 1.41 | +++ | +++ |
| 27 | 50 | 11 | 6.48 | -1.04 | -0.81 | -1.7 | +++ | +++ |
| 28 | 51 | 8.3 | 7.48 | -0.92 | -0.87 | -1.11 | +++ | +++ |
| 29 | 53 | 14 | 7.48 | -1.15 | -0.87 | -1.87 | +++ | +++ |
| 30 | 55 | 37 | 8.02 | -1.57 | -0.9 | -4.62 | ++ | +++ |
| 31 | 56 | 4.3 | 8.79 | -0.63 | -0.94 | 2.04 | +++ | +++ |
| 32 | 59 | 28 | 5.17 | -1.45 | -0.71 | -5.41 | ++ | +++ |
| 33 | 62 | 11 | 9.48 | -1.04 | -0.98 | -1.16 | +++ | +++ |
| 34 | 63 | 10 | 7.27 | -1 | -0.86 | -1.37 | +++ | +++ |
| 35 | 66 | 59 | 26.8 | -1.77 | -1.43 | -2.2 | ++ | +++ |
| 36 | 68 | 30 | 246 | -1.48 | -2.39 | 8.2 | +++ | + |
| 37 | 72 | 25 | 20.95 | -1.4 | -1.32 | -1.2 | +++ | +++ |
| 38 | 75 | 1700 | 642.62 | -3.23 | -2.81 | -2.64 | + | + |
| 39 | 77 | 310 | 301.95 | -2.49 | -2.48 | -1.02 | + | + |
| 40 | 81 | 14 | 8.52 | -1.15 | -0.93 | -1.64 | +++ | +++ |
| 41 | 84 | 6.9 | 4.3 | -0.84 | -0.63 | -1.6 | +++ | +++ |
| 42 | 87 | 19 | 12.36 | -1.28 | -1.09 | -1.54 | +++ | +++ |
| 43 | 88 | 240 | 73.92 | -2.38 | -1.87 | -3.25 | + | ++ |

^a Values in the error column represent the ratio of predicted to observed activity, or its negative inverse if the ratio is less than 1. ^b Activity scale: highly active (<50 nM, +++), moderately active (51–200 nM, ++), and less active (>200 nM, +).

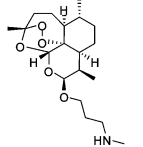
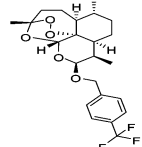
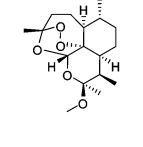
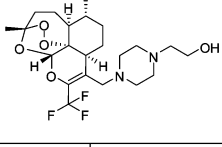
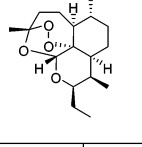
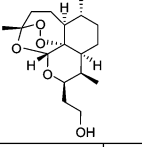
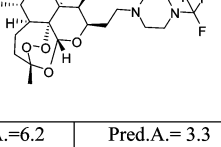
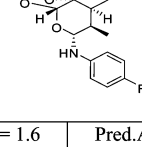
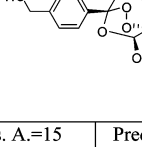
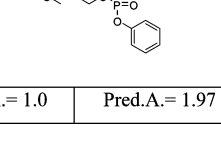
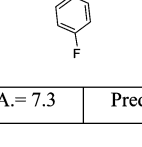
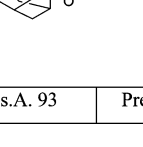
predictions. The other reason for the outlier behavior of these compounds may be due to their inability to achieve an energetically favorable conformation as well as the inter-feature distances (geometrical distance) between the important features found in the best pharmacophore.

2.5. Focused Virtual Library Screening. In silico screening is not restricted to commercial databases of existing compounds but can be performed with focused virtual libraries containing unknown compounds for new lead discovery, synthesis, and further lead optimization. The high extent of structural diversity, the high degree of drug likeness, and eventually the synthetic accessibility are among the criteria that may be useful for virtual library generation. Several methods to screen the focused virtual library with desired properties have been recently discussed in a review.³⁹ Among these methods, the fragment-based method for the generation of a focused virtual library has been used in our studies, using the software CombiGlide⁴⁰ which allows the user to a run fragment-based generation of a virtual library

in a user-friendly interface. The “Protocores” (Figure 7) consistent with 1,2,4-trioxane ring were considered for the library generation using the default parameter setting implemented in the CombiGlide.

A fragment set was prepared in the “Reagent Preparation Wizard” of the maestro panel of Schrödinger software, where among 41 different substitution reactions with reactants, the “R-I” type of reactants have been chosen for reagent preparation. Based on the pharmacophoric features requirement various hydrophobic substituent’s (R), viz., cyclohexane, cyclopentane, ethane, propane, butane, benzene, dimethylbenzene, trimethylbenzene, 2-methoxybenzene, *o*-tolylmethanol, *o*-tolylethanol, naphthalene, phenanthrene, indole, thiophene, coumaron, and benzisoxazole were drawn and used for the reagent preparation. The focused virtual library generation was carried out using “Combinatorial Library Enumeration” wizard of the maestro panel where the virtually prepared reagents were selectively added to attachment points “R1” and “R2” (Figure 7) which resulted into 600 new

Table 5. Structures of the Known Synthetic Trioxanes along with Their Observed and Predicted Activity Based on Hypo-1^a

| | | |
|---|---|---|
|  <p>A</p> |  <p>B</p> |  <p>C</p> |
| Obs.A.= 2.4 Pred. A.=18.6 | Obs.A.= 5.3 Pred.A.=0.6 | Obs.A.= 0.8 Pred.A.= 6.75 |
|  <p>D</p> |  <p>E</p> |  <p>F</p> |
| Obs.A.= 15.2 Pred. A.= 8.0 | Obs.A.= 1.0 Pred.A.= 6.0 | Obs.A.=1.9 Pred.A.= 16.4 |
|  <p>G</p> |  <p>H</p> |  <p>I</p> |
| Obs.A.=6.2 Pred.A.= 3.3 | Obs.A.= 1.6 Pred.A.= 0.11 | Obs. A.=15 Pred.A.= 36.22 |
|  <p>J</p> |  <p>K</p> |  <p>L</p> |
| Obs.A.= 1.0 Pred.A.= 1.97 | Obs.A.= 7.3 Pred.A.= 64.1 | Obs.A.= 93 Pred.A.= 274 |

^a Obs. A. = observed activity, and Pred. A. = predicted activity.**Table 6.** Observed and Predicted Activity of Clinically Active Trioxanes Based on Hypo-1

| serial no. | name | observed IC ₅₀ (nM) | predicted IC ₅₀ (nM) |
|------------|-------------|-----------------------------------|------------------------------------|
| 1 | artemisinin | 11 | 6.8 |
| 2 | artemether | 1.2 | 8.2 |
| 3 | arteether | 6.1 | 7.4 |
| 4 | artesunate | 1.6 | 6.7 |
| 5 | artelinate | — | 0.7 |
| 6 | artemiseone | 0.88 | 33.6 |

trioxanes. The whole process of the generation of a focused virtual library was carried out on a Red Hat Enterprise Linux (RHEL) 5 based Operating system having an Intel Pentium dual core 2.8 GHz processor. The generated virtual library was submitted to the build database protocol implemented in the Discovery Studio 2.0 (DS 2.0), which provided a multiconformer database. The 3D quantitative pharmacophore Hypo-1 was used to estimate the biological activities of the above database in DS 2.0, followed by a drug-likeness screen to ensure high drug-likeness of the compounds. On the basis of their predicted IC₅₀ values, the top 50 scoring molecules were considered as active new hits. In order to

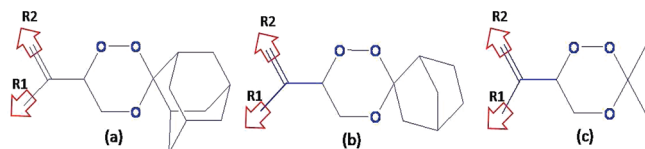
Table 7. Observed and Predicted Activity of Five Synthesized Trioxanes along with Standard Drugs Based on Hypo-1

| serial no. | compound | observed activity IC ₅₀ ^a (nM) | predicted activity IC ₅₀ (nM) | LogP |
|------------|-------------|---|---|-------|
| 1 | 5a | 35 ± 2.375 | 83.66 | 4.516 |
| 2 | 6a | 76 ± 5.88 | 18 | 4.444 |
| 3 | 6b | 85.40 ± 4.93 | 14.30 | 3.523 |
| 5 | 7a | 55.70 ± 4.42 | 20.68 | 4.796 |
| 6 | 7b | 47.70 ± 3.85 | 14.61 | 3.852 |
| 7 | artemether | 2.20 ± 0.13 | 8.20 | 2.422 |
| 8 | arteether | 2.84 ± 0.22 | 7.40 | 2.845 |
| 9 | chloroquine | 16.3 ± 1.10 | — | 5.875 |

^a IC₅₀: concentration corresponding to 50% growth inhibition of chloroquine sensitive strain 3D7 of *P. falciparum* (data are expressed as means ± SD from three different experiments in duplicate).

further evaluate the predictability of the pharmacophore model, five substituted 1,2,4-trioxanes among the top 50 scoring hits were synthesized and evaluated for their anti-malarial activity (Table 7).

2.6. Synthesis. Allylic alcohols (3a–c) were prepared from the corresponding ketones (1a–c) according to the reported procedure⁴¹ and were photo-oxygenated to give β-hydroxy hydroperoxides (4a–c). The photo-oxygenated products of allylic alcohols (β-hydroxy hydroperoxides) were not isolated and were condensed in situ, where 4a on condensation with 2-adamantanone gave trioxane 5a, while 4b and 4c in a similar reaction with norcamphor and acetone gave trioxanes 6a–b and 7a–b, respectively, in the presence of a catalytic amount of HCl to furnish these trioxanes with 49–58% overall yields.

**Figure 7.** Protocoresh (a,b and c) used in the focused virtual library generation. R1 and R2 denote the attachment points where prepared reagents have been selectively attached.

2.7. Biological Evaluation. All the five synthesized compounds along with the standard drug artemether, arteether, and chloroquine were evaluated for their in vitro antimalarial activity against chloroquine (CQ) sensitive 3D7 strain of *P. falciparum* BY SYBER green I-based fluorescence (MSF) assay⁴² (Table 7).

As shown in Table 7, the reported pharmacophore has been successfully applied in predicting the in vitro antimalarial activity of 1,2,4-trioxanes, where the error factor between estimated and experimental activity of the three molecules (viz., 5a, 7a, and 7b) out of five were ~ 3 (the uncertainty ratio of the CATALYST), while two molecules, viz., 6a and 6b have the error factor of 4.2 and 6, respectively.

The pharmacophore mapping experiment of the five synthesized compounds revealed that aliphatic substituents at position 3' of trioxane ring, viz., adamantyl, cycloheptane, and dimethyl groups, provided the HYAl functionality, while 2,5-dimethyl phenyl, phenyl, and 2-methoxy phenyl groups provided the HYAr functionality to the molecule. The trioxane ring itself provided the HBA and HBAL functionalities to the molecule. The active molecules (5a and 7b) among the five are simple trioxanes which contained the required pharmacophoric features.

To check the absorption, distribution, metabolism, and excretion (ADME)/toxicity of the synthesized compounds, the five synthesized compounds were submitted to the Moby server based program for ADME/toxicity filtration, where all the synthesized compounds passed these filtration criteria necessary for drug-likeness (<http://mobyle.rpbs.univ-paris-diderot.fr/cgi-bin/portal.py?form=admetox>).

The log *P* value in the water/octanol system has been calculated for all five synthesized trioxanes in the QuickProp protocol of Schrödinger software (Table 7), where it has been found that their Log *P* value is comparable with the most active molecule of the training set (molecule 40, Log *P* = 3.57) as well as some clinically active molecules. (viz., artelinate, Log *P* = 3.79; and arteether, Log *P* = 2.85). Further, all the five synthesized compounds were soluble in ethanol, dimethyl sulfoxide (DMSO), and dichloromethane (DCM).

In summary, the reported pharmacophore was found useful in the prediction of antimalarial activity of substituted 1,2,4-trioxanes with significantly high reliability, which provided a cost-effective and significant solution for identifying novel hits.

3. CONCLUSION

In the above study a quantitative pharmacophore model has been developed using a training set of 45 substituted 1,2,4-trioxanes. The best hypothesis consisted five features, viz., two HYAl, one HYAr, one HBA, and one HBAL with an excellent correlation ($r^2_{\text{training}} = 0.85$) for the training set and fair ($r^2_{\text{test}} = 0.51$) for test set of 43 substituted trioxanes. The model also well explained the observed antimalarial activity of known synthetic trioxanes as well as clinically effective antimalarial drugs. In order to further validate this model, five substituted 1,2,4-trioxanes were synthesized from the generated focused library and screened for antimalarial activity, where the observed activity of these molecules was consistent with the pharmacophore model. Accordingly, the

pharmacophore model may be useful in the design of substituted trioxanes as potent antimalarial agents.

4. EXPERIMENTAL SECTION

4.1. Pharmacophore Modeling. Pharmacophore generation was performed on a Windows-based operating system having an Intel Pentium dual core 2.8 GHz. processor using the HypoGen algorithm³² of CATALYST implemented in the Discovery Studio 2.0 software package (DS 2.0).⁴³ All compounds used in the QSAR study were built using ISIS Draw 2.5 and imported to DS 2.0 Windows, where the stereochemistry in the molecules was specified. These compounds were optimized using the CHARMM force field, and a maximum of 255 conformations were generated using the “best” conformational search, using the “Poling” algorithm⁴⁴ within an energy threshold of 20.0 kcal/mol with respect to the global minimum. A minimum number of 16 compounds is recommended for the training set for assured statistical power of the generated hypothesis with HypoGen algorithm.³¹ The important aspect of the training set compounds selection is that each active compound should provide new information to the HypoGen to help it uncover as much critical information as possible for predicting biological activity. The training set molecules associated with their conformations were submitted to the pharmacophore generation procedure (HypoGen).

HypoGen algorithm allows identification of hypotheses that are common to the “active” molecules in the training set but at the same time not present in the “inactives”.³² This algorithm allows a maximum of five features in the pharmacophore generation out of an inbuilt collection of 11, which are HBA, HBAL, HBD, HY, HYAl, HYAr, positively (PC) and negatively (NC) charged, positively (PI) and negatively (NI) ionizable, and ring aromatic (RA) features. Among these features available for selection, four features, viz., HBA, HBAL, HYAl, and HYAr present in the training set were selected for pharmacophore generation. Pharmacophore generation was carried out by using the default parameters and the setting implemented in the HypoGen generation procedure of the CATALYST except for the interfeature distance, where a default value (2.97 Å) was reduced to 2 Å due to small molecular size of the active compounds used in the training set. The choice and number of features used in the hypothesis construction were HBA (min. 1 – max. 5), HBAL (min. 1 – max. 5), HYAr (min. 1 – max. 5), and HYAl (min. 1 – max. 5). A default activity uncertainty value of 3 has been used in the pharmacophore generation. The specifications regarding the pharmacophore generation have been well documented by Kristam et al. to perform the reproducibility of the pharmacophore.⁴⁵

An uncertainty Δ in the CATALYST paradigm indicates an activity value lying somewhere in the interval from “activity divided by Δ ” to “activity multiplied by Δ ”. The resultant best 10 generated hypotheses were assessed on the basis of the cost relative to the null hypothesis and the correlation coefficients. The total cost value is the summation of weight, error, and a configuration cost value. The weight component is a value that increases in a Gaussian form because of the deviation of function weights from the ideal value of 2. Increase of the root-mean-square (rms) divergence between estimated and measured activity for the training set

molecules results in a higher error cost value. The configuration cost is a fixed cost that quantifies the entropy of the hypothesis space. In the standard HypoGen mode, the configuration cost should not exceed a maximum value of 17 (corresponds to a number of 2^{17} pharmacophore models) because high values may lead to chance correlation of the generated hypothesis, since CATALYST cannot consider more than 2^{17} models in the optimization phase, and so the rest are left out of the process. The HypoGen module performs two additional theoretical cost calculations (represented in bit units) to help the user in assessing the statistical significance of the generated hypothesis. The fixed cost is the lowest possible cost representing a hypothetical, simplest model that fits all data perfectly. It is calculated by adding the minimum achievable error, the weight cost, and the constant configuration cost. The null cost represents the maximum cost of a pharmacophore with no features and estimates activity to be the average of the training set molecule's activity data. Its absolute value is equal to the maximum occurring error cost. The statistical significance of the hypothesis increases when the total cost value is close to the fixed cost value and when the difference between null and total costs is high. The estimation of the activity of each training set compound is based on the regression analysis between the parameters computed by using the relationship of the geometric fit value versus the negative logarithm of activity, and so the higher the geometric fit value is, the greater the activity prediction is of the compound. The fit function does not depend only on the mapping of the feature but also contains a distance term measuring the distance between the feature on the molecule and the centroid of the hypothesis feature, and both these terms are used in the calculation of geometric fitness. The method has been documented to perform better than a structure-based pharmacophore generation.^{46,47}

4.2. Chemistry. Melting points were determined in open capillaries on a COMPLAB melting point apparatus and are uncorrected. IR spectra were recorded on a Perkin-Elmer RXI FT-IR spectrophotometer. ^1H NMR was recorded on a Bruker Supercon Magnet DPX-200 (operating at 200 MHz for ^1H) spectrometer using CDCl_3 as the solvent. Tetramethylsilane (0.00 ppm) served as an internal standard in ^1H NMR. Multiplicities are represented by s (singlet), d (doublet), dd (doublet of doublet), t (triplet), q (quartet), bs (broad singlet), and m (multiplet). High-resolution electron impact mass spectra (HR-EIMS) were obtained on a JEOL JMS-600H instrument. For all trioxanes, satisfactory high-resolution mass spectra were obtained, confirming purity. Reactions were monitored on silica gel thin-layer chromatography (TLC) plates. Column chromatography was performed over silica gel (60–120 mesh) procured from Qualigens (India) using freshly distilled solvents. All the chemicals and reagents were obtained from Aldrich (USA), Lancaster (England), or Spectrochem (India) and were used without purification.

4.3. Trioxane 5a. 3-(2-Methoxyphenyl)but-2-en-1-ol (1 g) was dissolved in acetonitrile (60 mL) in a double-jacketed round-bottomed flask assembled with a cryostat (instrument used for maintaining low temperature between -10 and 0°C) and methylene blue (10 mg) was added. The reaction mixture was irradiated with a tungsten halogen filament lamp (500 W), and oxygen was bubbled into the reaction mixture

for 10 h. The crude product β -hydroxy hydroperoxide obtained was directly subjected to condensation with 2-adamantanone (2.6 mL) in CH_3CN (80 mL) and CH_2Cl_2 and 1–2 drops of conc. HCl were added, and the reaction mixture was stirred for 2.5 h at room temperature. The reaction mixture was concentrated to yield 3.81 g of the crude product. It was chromatographed on silica gel (150 g) using EtOAc:hexane, (0.5:99.5) as an eluent to furnish 2.37 g (58% yield, based on allylic alcohol) pure trioxane 5a as a white solid (mp = 58°C).

Trioxanes 6a–b were prepared from allylic alcohols 3b, while trioxanes 7a–b were prepared from allylic alcohols 4b in a similar way by replacing 2-adamantanone with norcamphor (560 mg, for trioxane 6a and 7a) and acetone (5 mL, for trioxane 6b and 7b), respectively.

4.4. Trioxane 5a. Yield 58%, white solid, mp = 57 – 59°C , FT-IR (KBr, cm^{-1}) 3460.7, 2361.5, 1597.9, 1458.2, 1245.6, 1109.3, 1000.7, 917, 757; ^1H NMR (2918.2, 300 MHz, CDCl_3), δ 1.57–2.09 (m, 13H), 2.96 (bs, 1H), 3.81 (dd, 1H, J = 11.8 and 3.3 Hz), 3.85 (s, 3H), 3.92 (dd, 1H, J = 11.8 and 10.3 Hz), 5.2 (dd, 1H, J = 10.3 and 2.3 Hz), 5.33 (s, 1H), 5.43 (s, 1H), 6.89–6.95 (m, 2H), 7.13–7.16 (m, 1H), 7.29–7.35 (m, 1H); ESMS (m/z): 343.1 $[\text{M} + \text{H}]^+$; HRMS for fragment ion $[\text{M} + 2\text{H}]^{2+}$ $\text{C}_{21}\text{H}_{28}\text{O}_4$: 344.1979 (obs.); 344.1988 (calcd.).

4.5. 6'-(1-(2,4-Dimethylphenyl)vinyl)spiro[bicyclo[2.2.1]heptane-2,3'-[1,2,4]trioxane] (6a). Yield 55%, yellow liquid FT-IR (KBr, cm^{-1}) 3015.3, 2966.9, 2874.0, 2362.1, 1450.8, 1328.6, 1217.5, 1132.3, 1105.8, 1055.1, 968.6, 824.2, 760.1, 669.2; ^1H NMR (300 MHz, CDCl_3), δ 1.27–1.80 (m, 10H), 2.28 (s, 3H), 2.33 (s, 3H), 3.60–3.88 (m, 2H), 4.89–5.01 (m, 1H), 5.15 (s, 1H), 5.44 (s, 1H), 6.94–7.35 (m, 3H); ESMS (m/z): 300.4 $[\text{M}]^+$; HRMS for fragment ion $[\text{M} + \text{H}]^{1+}$ $\text{C}_{19}\text{H}_{25}\text{O}_3$: 301.1785 (obs.); 301.1804 (calcd.).

4.6. 6-(1-(2,4-Dimethylphenyl)vinyl)-3,3-dimethyl-1,2,4-trioxane (6b). Yield 49%, Yellow liquid; FT-IR (KBr, cm^{-1}) 3428.8, 3018.8, 2927.4, 2361.2, 1612.3, 1449.9, 1376.5, 1215.0, 1162.0, 1049.9, 927.6, 760.7, 669.8; ^1H NMR (200 MHz, CDCl_3), δ 1.36 (s, 3H), 1.63 (s, 3H), 2.26 (s, 3H), 2.31 (s, 3H), 3.687 (dd, 1H, J = 11.84 and 3 Hz), 3.87 (dd, 1H, J = 11.87 and 10.2 Hz), 4.93 (dd, J = 10.24 and 2.82 Hz), 5.17 (s, 1H), 5.47 (s, 1H), 6.96–7.26 (m, 3H); ESMS (m/z): 247.2 $[\text{M} - \text{H}]^-$; HRMS for fragment ion $\text{C}_{15}\text{H}_{19}\text{O}_3$ $[\text{M} - \text{H}]^-$ 247.1307 (obs.); 247.1334 (calcd.).

4.7. (Z)-6'-(1-Phenylpent-1-enyl)spiro[bicyclo[2.2.1]heptane-2,3'-[1,2,4]trioxane] (7a). Yield 56%, Yellow liquid, FT-IR (KBr, cm^{-1}) 3020.4, 2963.2, 2361.7, 1680.9, 1647.7, 669.5, 1328, 1216, 1107.3, 762.0; ^1H NMR (300 MHz, CDCl_3), δ 0.97 (t, 3H, J = 7.26 Hz), 1.27–1.79 (m, 12H), 2.34–2.39 (m, 2H), 3.52–3.87 (m, 2H), 5.41–5.51 (m, 1H), 5.84 (t, 1H, J = 7.53 Hz), 7.47–7.99 (m, 5H); ESMS (m/z): 315.2 $[\text{M} + \text{H}]^+$; HRMS for fragment ion $[\text{M} - \text{H}]^-$ $\text{C}_{20}\text{H}_{25}\text{O}_3$: 313.1811 (obs.); 313.1804 (calcd.).

4.8. (Z)-3,3-Dimethyl-6-(1-phenylpent-1-enyl)-1,2,4-trioxane (7b). Yield 52%, Yellow liquid, FT-IR (KBr, cm^{-1}) 3376.0, 3019.6, 2962.2, 2873.5, 1732.1, 1374.9, 1215.4, 1161.4, 1048.7, 903.1, 759.5, 668.4; ^1H NMR (300 MHz, CDCl_3), δ 1 (t, 3H, J = 7.32 Hz), 1.39 (s, 3H), 1.49–1.57 (m, 2H), 1.61 (s, 3H), 2.33–2.41 (m, 2H), 3.53 (dd, 1H, J = 12 and 3 Hz), 3.93 (dd, 1H, J = 11.94 and 11.1 Hz), 5.42 (dd, 1H, J = 11 and 3 Hz), 5.82 (t, 1H, 7.59 Hz), 7.28–7.35

(m, 5H); ESMS (m/z): 261.1[M - H]⁻; HRMS for C₁₆H₂₂O₃: 262.1548(obs.); 262.1569 (calcd.).

Biological Testing. The compounds were dissolved in DMSO at 5 ng/mL. For the assays, fresh dilutions of all compounds in the screening medium were prepared, and 50 μ L of highest starting concentration (500 ng/mL) was dispensed in duplicate wells in row "B" of 96 well tissue culture plates. The highest concentration for chloroquine was 25 ng/mL. Subsequently two-fold serial dilutions were prepared up to row "H" (seven concentrations). Finally 50 μ L of a 2.5% parasitized cell suspension containing 0.5% parasitaemia was added to each well except four wells in row "A" which received non infected cell suspension. These wells containing noninfected erythrocytes in the absence of drugs served as negative controls, while parasitized erythrocytes in the presence of CQ served as positive controls. After 72 h of incubation, 100 μ L of lysis buffer [20 mM tris (pH 7.5), 5 mM EDTA, 0.008% (wt/vol) saponin, and 0.08% (v/v) Triton X-100] containing one times the concentration of SYBER green I (Invitrogen) was added to each cell. The plates were reincubated for 1 h at room temperature and examined for the relative fluorescence units (RFUs) per well using the FLUO star, BMG lab technologies. The IC₅₀ has been determined using nonlinear regression analysis dose response curves. It is worthwhile to note that the standard deviation (SD) in the measurement of the IC₅₀ value for five synthesized compounds along with standard drugs artemether, arteether, and chloroquine was an average of 7% of the mean, which is comparable with the SD in the measurement of IC₅₀ value (8–10% of the mean) for the training and test sets considered for QSAR study.

ACKNOWLEDGMENT

The authors are thankful to Mrs. S. Rastogi, Mr. A. K. Srivastava, and Mr. A. S. Kushwaha for the technical assistance and to SAIF and CDRI, Lucknow, for providing spectroscopic data. Two of authors (A.K.G. and S.C.) acknowledge CSIR, New Delhi, for financial support.

Supporting Information Available: Schemes for the syntheses of trioxane 5a, 6a-b and 7a-b, ¹H NMR spectra of trioxane 5a, 6a-b and 7a-b and 3D structures of all the molecules used in the QSAR study in their best scoring conformations in the SDF format. This material is available free of charge via the Internet at <http://pubs.acs.org>.

REFERENCES AND NOTES

- (1) Aregawi, M.; Williams, R.; Dye, C.; Cibulskis, R.; Otten, M. World Malaria Report 2008; World Health Organization (WHO): Geneva, Switzerland, 2008.
- (2) Rosenthal, A. S.; Chen, X.; Liu, J. O.; West, D. C.; Hergenrother, P. J.; Shapiro, T. A.; Posner, G. H. Malaria-Infected Mice are Cured by a Single Oral Dose of New Dimeric Trioxane Sulfones Which are also Selectively and Powerfully Cytotoxic to Cancer Cells. *J. Med. Chem.* **2009**, *52*, 1198–1203.
- (3) Snow, R. W.; Guerra, C. A.; Noor, A. M.; Myint, H. Y.; Hay, S. I. The Global Distribution of Clinical Episodes of *Plasmodium falciparum* Malaria. *Nature* **2005**, *434*, 214–217.
- (4) Antimalarial drug resistance. In *Antimalarial Chemotherapy: Mechanisms of Action, Resistance, and New Directions in Drug Discovery*; Rosenthal, P. J., Ed.; Humana Press: Totowa, NJ, 2001; pp 65–83.
- (5) Wright, C. W. Traditional Antimalarials and the Development of Novel Antimalarial Drugs. *J. Ethnopharmacol.* **2005**, *100*, 67–71.
- (6) Klayman, D. L. Qinghaosu (Artemisinin) An Antimalarial Drug from China. *Science* **1985**, *228*, 1049–1055.
- (7) Ploypradith, P. Development of Artemisinin and its Structurally Simplified Trioxane Derivatives as Antimalarial Drugs. *Acta Trop.* **2004**, *89*, 329–342.
- (8) White, N. J. Qinghaosu (Artemisinin): The Price of Success. *Science* **2008**, *320*, 330–334.
- (9) Afonso, A.; Hunt, P.; Cheeseman, S.; Alves, A. C.; Cunha, C. V.; Rosario, V. do; Carvo, P. Malaria Parasites can Develop Stable Resistance to Artemisinin but Lack Mutations in Candidate Genes *atp6* (Encoding the Sarcoplasmic and Endoplasmic Reticulum Ca²⁺-ATPase), *tctp*, *mdr1* and *cg10*. *Antimicrob. Agents Chemother.* **2006**, *50*, 480–489.
- (10) Noedl, H.; Se, Y.; Schaefer, K.; Smith, B. L.; Socheat, D.; Fukuda, M. M. Evidence of Artemisinin-Resistant Malaria in Western Cambodia. *N. Engl. J. Med.* **2008**, *359*, 2619–2620.
- (11) Maude, R. J.; Pontavornpinyo, W.; Saralamba, S.; Aguas, R.; Yeung, S.; Dondorp, A. M.; Day, N. P. J.; White, N. J.; White, L. J. The Last Man Standing is the Most Resistant: Eliminating Artemisinin Resistant Malaria in Cambodia. *Malaria J.* **2009**, *8*, 31.
- (12) O'Neill, P. M.; Posner, G. H. A Medicinal Chemistry Perspective on Artemisinin and Related Endoperoxides. *J. Med. Chem.* **2004**, *47*, 2945–2964.
- (13) Posner, G. H.; O'Neill, P. M. Knowledge of the Proposed Chemical Mechanism of Action and Cytochrome P450 Metabolism of Antimalarial Trioxanes Like Artemisinin Allows Rational Design of New Antimalarial Peroxides. *Acc. Chem. Res.* **2004**, *37*, 97–104.
- (14) Ueckstein-Ludwig, R. J.; Web, I. D. A.; Van Goethem, J. M.; East, A. G.; Lee, M. K. P. G.; Bray, S. A.; Ward, S. K. Artemisinins Target the SERCA of *Plasmodium falciparum*. *Nature* **2004**, *424*, 957–961.
- (15) Posner, G. H.; Chang, W.; Hess, L.; Woodard, L.; Sinishtaj, S.; Usera, A. R.; Maio, W.; Rosenthal, A. S.; Kalinda, A. S.; D'Angelo, J. G.; Petersen, K. S.; Stohle, R.; Chollet, J.; Santo-Tomas, J.; Snyder, C.; Rottmann, M.; Wittlin, S.; Brun, R.; Shapiro, T. A. Malaria-Infected Mice are Cured by Oral Administration of New Artemisinin Derivatives. *J. Med. Chem.* **2008**, *51*, 1035–1042.
- (16) O'Neill, P. M.; Mukhtar, A.; Ward, S. A.; Bickley, J. F.; Davies, J.; Bachi, M. D.; Stocks, P. A. Application of Thiol-Olefin Cooxygenation Methodology to a New Synthesis of the 1,2,4-Trioxane Pharmacopoeia. *Org. Lett.* **2004**, *18*, 3035–3038.
- (17) Cabaret, O. D.; Vical, F. B.; Loup, C.; Robert, A.; Gornitzka, H.; Bonhoure, A.; Vial, H.; Magnaval, J. F.; Seguela, J. P.; Meunier, B. Synthesis and Antimalarial Activity of Trioxaquinones Derivatives. *Chem.-Eur. J.* **2004**, *10*, 1625–1636.
- (18) Griesbeck, A. G.; El-Idreesy, T. T.; Höinck, L. O.; Lex, J.; Brun, R. Novel Spiroannelated 1,2,4-Trioxanes with High *in vitro* Antimalarial Activities. *Bioorg. Med. Chem. Lett.* **2005**, *15*, 595–597.
- (19) Singh, C.; Verma, V. P.; Naikade, N. K.; Singh, A. S.; Hassam, M.; Puri, S. K. Novel Bis- and Tris-1, 2, 4-trioxanes: Synthesis and Antimalarial Activity Against Multidrug-Resistant *Plasmodium yoelii* in Swiss Mice. *J. Med. Chem.* **2008**, *51*, 7581–7592.
- (20) Vennerstrom, S. J. L.; Brun, A. B. R.; Charman, S. A.; Chlu, F. C. K.; Chollet, J.; Dong, Y.; Dorn, A.; Hunziker, D.; Matile, H.; McIntosh, K.; Padmanilayam, M.; Tomas, J. S.; Scheurer, C.; Scorneaux, B.; Tang, Y.; Urwyler, H.; Wittlin, S.; Charman, W. N. Identification of an Antimalarial Synthetic Trioxolane Drug Development Candidate. *Nature* **2004**, *430*, 900–904.
- (21) Uhlemann, A. C.; Wittlin, S.; Matile, H.; Bustamante, L. Y.; Krishna, S. Mechanism of Antimalarial Action of the Synthetic Trioxolane, RBX11160 (OZ277). *Antimicrob. Agents Chemother.* **2007**, *51*, 667–672.
- (22) Jung, M.; Kim, H. CoMFA of Artemisinin Derivatives: Effect of Location and Size of Lattice. *Bioorg. Med. Chem. Lett.* **2001**, *11*, 2041–2044.
- (23) Avery, M. A.; Gaston, M. A.; Rodrigues, C. R.; Barreiro, E. J.; Cohen, F. E.; Sabnis, Y. A.; Woolfrey, J. R. Structure-Activity Relationships of the Antimalarial Agent Artemisinin: The Development of Predictive *in vitro* Potency Models Using CoMFA and HQSAR Methodologies. *J. Med. Chem.* **2002**, *45*, 292–303.
- (24) Grigorov, M.; Weber, J.; Tronchet, J. M. J.; Jefford, C. W.; Millhous, W. K.; Maric, D. A QSAR Study of the Antimalarial Activity of Some Synthetic 1, 2, 4-Trioxanes. *J. Chem. Inf. Comput. Sci.* **1997**, *37*, 124–130.
- (25) Egan, T. J. Artemisinin-Resistant *Plasmodium falciparum*: Can the Genie be Put Back in the Bottle. *Future Microbiol.* **2009**, *4*, 637–639.
- (26) Posner, G. H.; Park, S. B.; Gonzales, L.; Wang, D.; Cumming, J. N.; Klinedinst, D.; Shapiro, T. A.; Bachi, M. D. Evidence for the Importance of High-Valent Fe=O and of a di Ketone in the Molecular Mechanism of Action of Antimalarial Trioxane Analogs of Artemisinin. *J. Am. Chem. Soc.* **1996**, *118*, 3537–3538.
- (27) Posner, G. H.; Cumming, J. N.; Woo, S. H.; Ploypradith, P.; Xie, S.; Shapiro, T. A. Orally Active Antimalarial 3-Substituted Trioxanes: New Synthetic Methodology and Biological Evaluation. *J. Med. Chem.* **1998**, *41*, 940–951.

- (28) Cumming, J. N.; Wang, D.; Park, S. B.; Shapiro, T. A.; Posner, G. H. Design, Synthesis, Derivatization, and Structure-Activity Relationships of Simplified, Tricyclic, 1,2,4-Trioxane Alcohol Analogues of the Antimalarial Artemisinin. *J. Med. Chem.* **1998**, *41*, 952–964.
- (29) Posner, G. H.; O'Dowd, H.; Caferro, T.; Cumming, J. N.; Ploypradith, P.; Xie, S.; Shapiro, T. A. Antimalarial Sulfone Trioxanes. *Tetrahedron Lett.* **1998**, *39*, 2273–2276.
- (30) Posner, G. H.; Parker, M. H.; Northrop, J.; Elias, J. S.; Ploypradith, P.; Xie, S.; Shapiro, T. A. Orally Active, Hydrolytically Stable, Semisynthetic, Antimalarial Trioxanes in the Artemisinin Family. *J. Med. Chem.* **1999**, *42*, 300–304.
- (31) O'Dowd, H.; Ploypradith, P.; Xie, S.; Shapiro, T. A.; Posner, G. H. Antimalarial Artemisinin Analogs. Synthesis via Chemoselective C-C Bond Formation and Preliminary Biological Evaluation. *Tetrahedron.* **1999**, *55*, 3625–3636.
- (32) Gund, P. In *Pharmacophore Perception, Development, and Drug Design*; Gunner, O. F., Ed.; International University Line: La Jolla, CA, 2000; pp 3–11.
- (33) Kim, S. G.; Yoon, C.; Kim, S.; Cho, Y.; Kang, D. Building a Common Feature Hypothesis for Thymidylate Synthase Inhibition. *Bioorg. Med. Chem.* **2000**, *8*, 11–17.
- (34) Wei, N.; Sadzadeh, S. M. Enhancement of Hemin-Induced Membrane Damage by Artemisinin. *Biochem. Pharmacol.* **1994**, *48*, 737–41.
- (35) *The Principle of Experimentation Illustrated by a PsychoPhysical Experiment*, 8th ed.; Fischer, R., Ed.; Hafner Publishing Co.: New York, 1966.
- (36) Schlitzer, M. Malaria Chemotherapeutics Part I: History of Antimalarial Drug Development, Currently Used Therapeutics and Drugs in Clinical Development. *ChemMedChem.* **2007**, *2*, 944–986.
- (37) Snyder, C.; Cholleta, J.; Santo-Tomasa, J.; Scheurera, C.; Wittlin, S. In vitro and in vivo Interaction of Synthetic Peroxide RBx11160 (OZ277) with Piperaquine in Plasmodium Models. *Exp. Parasitol.* **2007**, *115*, 296–300.
- (38) Vivas, L.; Rattray, L.; Stewart, L. B.; Robinson, B. L.; Fugmann, B.; Haynes, R. K.; Peters, W.; Croft, S. L. Antimalarial Efficacy and Drug Interactions of the Novel Semi-Synthetic Endoperoxide Artemisone *in vitro* and *in vivo*. *J. Antimicrob. Chemother.* **2007**, *59*, 658–665.
- (39) Langer, T.; Krovat, E. M. Chemical Feature-Based Pharmacophores and Virtual Library Screening for Discovery of New Leads. *Curr. Opin. Drug Discovery Dev.* **2003**, *6*, 370–376.
- (40) *CombiGlide*, version 2.5; Schrödinger, LLC: New York, 2009.
- (41) Singh, C.; Kanchan, R.; Srivastava, D.; Puri, S. K. 8-(1-Naphthalen-2-yl-vinyl)-6, 7, 10-Trioxaspiro (4,5)Decane, a New 1,2,4-Trioxane Effective Against Rodent and Simian Malaria. *Bioorg. Med. Chem. Lett.* **2006**, *16*, 584–586.
- (42) Smilkstein, M.; Sriwilaijaroen, N.; Kelly, J. X.; Wilairat, P.; Riscoe, M. Simple and Inexpensive Fluorescence-Based Technique for High-Throughput Antimalarial Drug Screening. *Antimicrob. Agents Chemother.* **2004**, *48*, 1803.
- (43) *Discovery Studio*, version 2.0; Accelrys Software Inc.: San Diego, CA 2001.
- (44) Smellie, A.; Teig, S. L.; Poling, T. P. Promoting Conformational Variation. *J. Comput. Chem.* **1995**, *16*, 171–187.
- (45) Kristam, R.; Gillet, V. J.; Lewis, R. A.; Thorner, D. Comparison of Conformational Analysis Techniques to Generate Pharmacophore Hypotheses Using Catalyst. *J. Chem. Inf. Model.* **2005**, *45*, 461–476.
- (46) Greenidge, P. A.; Weiser, J. A Comparison of Methods for Pharmacophore Generation with the Catalyst Software and Their Use for 3D-QSAR: Application to a Set of 4-Aminopyridine Thrombin Inhibitors. *Mini-Rev. Med. Chem.* **2001**, *1*, 79–87.
- (47) Bhattacharjee, A. K.; Hartell, M. G.; Nichols, D. A.; Hicks, R. P.; Stanton, B. Structure-Activity Relationship Study of Antimalarial Indolo [2,1-b]Quinazoline-6,12-Diones (Tryptanthrins). Three-Dimensional Pharmacophore Modeling and Identification of New Antimalarial Candidates. *Eur. J. Med. Chem.* **2004**, *39*, 59–67.

CI100180E